Applied Surface Science 365 (2016) 153–159

Contents lists available at ScienceDirect

Applied Surface Science

journal homepage: www.elsevier.com/locate/apsusc

Laser textured superhydrophobic surfaces and their applications for homogeneous spot deposition

Van Duong Ta[a,*], Andrew Dunn[a], Thomas J. Wasley[b], Ji Li[b], Robert W. Kay[b], Jonathan Stringer[c], Patrick J. Smith[c], Emre Esenturk[d], Colm Connaughton[d,e], Jonathan D. Shephard[a]

[a] Institute of Photonics and Quantum Sciences, Heriot-Watt University, Edinburgh EH14 4AS, UK
[b] Additive Manufacturing Research Group, Loughborough University, Leicestershire LE11 3TU, UK
[c] Laboratory of Applied Inkjet Printing, Department of Mechanical Engineering, University of Sheffield, Sheffield S1 4BJ, UK
[d] Warwick Mathematics Institute, Zeeman Building, University of Warwick, Coventry CV4 7AL, UK
[e] Centre for Complexity Science, Zeeman Building, University of Warwick, Coventry CV4 7AL, UK

ARTICLE INFO

Article history:
Received 26 October 2015
Received in revised form
16 December 2015
Accepted 4 January 2016
Available online 6 January 2016

Keywords:
Superhydrophobic surface
Nanosecond laser texturing
Coffee-stain effect
Suppression of the coffee-stain effect
Stainless steel

ABSTRACT

This work reports the laser surface modification of 304S15 stainless steel to develop superhydrophobic properties and the subsequent application for homogeneous spot deposition. Superhydrophobic surfaces, with steady contact angle of ~154° and contact angle hysteresis of ~4°, are fabricated by direct laser texturing. In comparison with common pico-/femto-second lasers employed for this patterning, the nanosecond fiber laser used in this work is more cost-effective, compact and allows higher processing rates. The effect of laser power and scan line separation on surface wettability of textured surfaces are investigated and optimized fabrication parameters are given. Fluid flows and transportations of polystyrene (PS) nanoparticles suspension droplets on the processed surfaces and unprocessed wetting substrates are investigated. After evaporation is complete, the coffee-stain effect is observed on the untextured substrates but not on the superhydrophobic surfaces. Uniform deposition of PS particles on the laser textured surfaces is achieved and the deposited material is confined to smaller area.

1. Introduction

Superhydrophobic surfaces, for which the water contact angle is higher than 150°, have attracted increasing research interest due to the many potential applications ranging from biological to industrial processes and even in daily life [1–3]. Generally, a certain surface roughness is required to achieve these low wettability substrates [4,5] and various techniques for attaining them have been investigated, such as lithography, etching, deposition and laser processing [6]. Among these alternatives, laser texturing is a promising method due to the excellent control of surface roughness from nano- to micro-scale, single-step processing under ambient conditions and the ability to work with a large range of materials [7–10].

Direct patterning of superhydrophobic metallic surfaces by a femtosecond laser has been investigated [11,12], which is important for advanced printing techniques [13] and overcoming surface conductivity [14]. However, most of the reported works on controlling wettability of metals to date still rely on the use of pico-/femto-second lasers [15–22]. For industrial applications, there is high demand to reduce the costs by replacing the currently used, expensive, ultrafast lasers to more compact and cost-effective systems such as nanosecond fiber lasers [23].

It is well-known that the contact line between a droplet and a solid surface depends on the droplet contact angle. The higher the contact angle is, the smaller the contact line hence the droplet contact line is significantly reduced for droplets on superhydrophobic surfaces compared with that on typical hydrophobic or hydrophilic surfaces. Additionally, the surface-pinned contact line is strongly responsible for the coffee-stain effect [24]. Therefore, during evaporation of a droplet containing suspended particles, superhydrophibicity is expected to deposit the particles in an area with dimensions much smaller than would be achieved on a wetting surface and smaller than the original droplet size. Experimental realization of this effect will offer the possibility of using non-wetting surfaces for uniform coating and increasing resolution of inkjet printing.

* Corresponding author.
E-mail address: d.ta@hw.ac.uk (V.D. Ta).

http://dx.doi.org/10.1016/j.apsusc.2016.01.019

This work demonstrates the generation of superhydrophobic surfaces on 304S15 stainless steel by nanosecond laser texturing and their applications for homogenous deposition.

2. Methods and materials

2.1. Materials

Stainless steel (304S15, RS components) sheets (1 mm thick) were used for all experiments. These samples were cleaned with isopropanol prior to laser processing.

2.2. Laser surface irradiation

The laser source was a nanosecond fiber SPI laser (20W EP-S) with wavelength of 1064 nm. This laser was connected to a galvanometer scanner and F-Theta focusing lens for delivering a focused laser beam over the sample surface with nominal beam spot of 21 μm (defined as $1/e^2$ of maximum intensity of beam profile). The beam profile has a Gaussian shape with $M^2 = 1.1$. A pulse duration of ~220 ns and repetition rate of 25 kHz were used for all fabrication processes. Microstructures on the samples were created by scanning the laser beam with a fixed speed of 150 mm/s, first in x and then in y directions. The distance between adjacent laser scanning lines, the so-called scan line separation or pitch size, was kept constant for both paths. This distance will be referred as a, and has been indicated in Fig. 1e.

Surface morphology and wettability of laser processed surfaces were characterized as a function of laser fluence. The laser fluence is the ratio between laser pulse energy and laser beam area.

2.3. Surface characterization

The morphology of the laser structured surface was characterized by a scanning electron microscope (SEM), model FEI Quanta FEG650, and an optical microscope (Leica DM6000M). Three-dimensional (3D) profiles of laser processed surfaces were obtained by the Leica microscope. This was possible by using z-stack measurements supported from Leica Application Suite Version 4.2.0 (LAS V4.2). Surface roughness was characterized on an area of 450 μm × 600 μm (0.27 mm^2) and the LAS 4.2 provided the arithmetic mean of surface roughness based on the 3D profile obtained. Three individual measurements were performed on three different samples fabricated under exactly the same conditions with the presented surface roughness values (S_a) calculated by taking mean of the three values.

The surface wettability of as-received and laser structured samples was qualified by the contact angle (θ) of ~5 μL deionized water droplets deposited on the surface. The contact angle was obtained by analyzing droplet images (captured by a Unibrain 1394 camera) using the software FTA32 (version 2.0). Furthermore, contact angle hysteresis (CAH) was determined by subtracting the advancing and receding contact angles [11].

2.4. Preparation of polystyrene suspension

Polystyrene (PS) suspension (~0.08% solids) was used to demonstrate the coffee-stain effect. This was obtained by diluting the 2% solids PS monodisperse aqueous suspension (particle size of 0.5 μm, Sigma–Aldrich) with deionized water.

3. Results and discussion

3.1. Effect of laser radiation on surface morphology

Fig. 1 shows clearly the effect of laser irradiation on creating rough structures on the surfaces of the samples. As shown in Fig. 1a, the as-received substrate has a relatively smooth surface (S_a ~ 0.46 μm) and no hierarchical structure. During processing, the laser both moves and removes material from the surface via melting and evaporation (ablation) respectively, forming periodic structures. The surface morphology of textured surfaces depends on the laser power and the scan line separation. For a small line separation of 10 μm, the beam overlap between two adjacent lines is high (~65%) so the multi-directional structure is not well pronounced (Fig. 1b). In contrast, for a separation of 25 μm or larger (Fig. 1c and d) these additional structures are clearly observed. In addition, the pulse overlap (~79%) in a single scanning line is also visible in both x and y directions (Fig. 1d). In this work, we focused on a = 50 μm (Fig. 1e) as it is an optimized value which will be discussed later. For the 50 μm spacing, the line separation was sufficiently large that a proportion of the surface was not ablated. High-magnification of a single unit is presented in Fig. 1f where the unprocessed part is surrounded by evaporative micro-structures.

As mentioned earlier, the surface morphology depends on the laser power. Fig. 2a–d show SEM images of the structures with the same line separation of 50 μm and irradiated with various laser fluences. The depth of the structures increases and the heat zone expands with increasing fluence. The width of laser treated lines was only ~12 μm for a fluence of 25 J/cm^2, increasing significantly for higher irradiated energies. Heat zones of 21, 29 and 35 μm were measured for a fluence of 33, 40 and 48 J/cm^2, respectively.

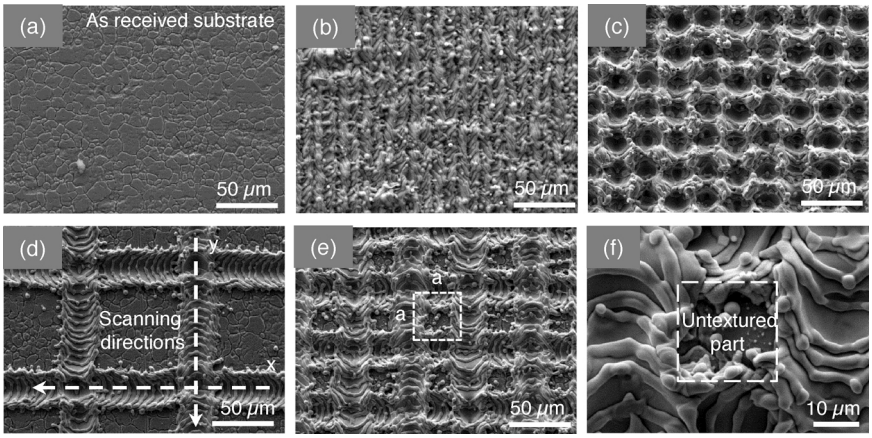

Fig. 1. SEM images of the original, as-received surface and laser textured surfaces irradiated with the same fluence of 36 J/cm^2. (a) As-received stainless steel (304S15) substrate. (b–d) The line separations are 10, 25 and 100 μm, respectively. (e) Structures with line separation of 50 μm and (f) high-resolution of a single unit.

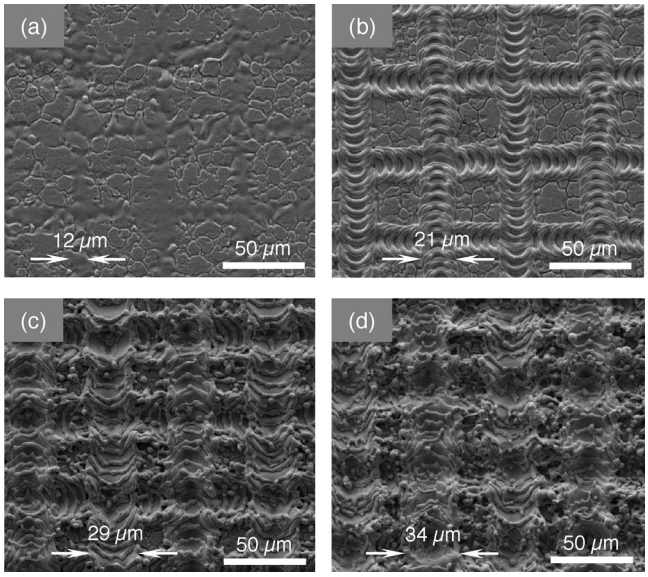

Fig. 2. SEM images of laser textured surfaces irradiated with the same line separation of 50 μm for various powers. (a)–(d) Laser fluence of 25, 33, 40, 48 J/cm^2, respectively.

Generally, the heat zone expanded three times when the laser fluence was doubled. To get more information about surface roughness an optical microscope was used to study these samples. Fig. 3a shows the 3D profile of a typical surface, irradiated with 36 J/cm^2. The created structures have an average depth of ~7 μm with depths of up to ~11 μm achieved where laser processed lines cross.

Surface roughness measurements were carried out on three separate samples for each fluence and the results are shown in Fig. 3b. The roughness of the laser textured surfaces for fluences below and around 33 J/cm^2 was not significantly higher than the value of 0.46 μm measured for the unprocessed surface. However, the S_a increased linearly with fluences higher than 33 J/cm^2. The roughness was around 2 and 7 times greater compared with that of the untextured surface for fluences of 36 and 48 J/cm^2, respectively. The result shows that surface roughness can be well-controlled by laser power.

3.2. Effect of exposure time to ambient conditions on surface wettability

The surface wettability of laser textured surfaces changed over time when exposed to ambient conditions (temperature of 22–24 °C and relative humidity of ~44%). Fig. 4a plots the contact angle of a laser structured surface (a = 50 μm, 36 J/cm^2) as function of time. Shortly after fabrication, the contact angle was relatively small; around 10° after being left in the air for one day. However, the contact angle gradually increased with time. After 13 days it was ~152° and it reached a stable value of ~154° by day 18, after which no significant change in the contact angle was observed. Furthermore, we have measured the contact angle of laser processed surfaces (a = 50 μm) that were irradiated with laser fluences higher than 36 J/cm^2 and left under ambient conditions for ~6 months. The results are shown in Fig. S1. It was found that the contact angle is ~155° for all fluences from 36 to 48 J/cm^2. That means after reaching the steady state, there is no difference in the evolution of surface wettability (in terms of contact angle) with time for surfaces irradiated with different laser fluences.

The above phenomenon has been reported previously [12]. Directly after fabrication, the laser structured surfaces were hydrophilic primarily because the laser-induced roughness amplified the wetting behavior of these surfaces according to Wenzel's model [4]. However, the change of wettability over time is due to modification of surface chemistry and the decomposition of carbon dioxide into carbon with active magnetite can be a key factor [12].

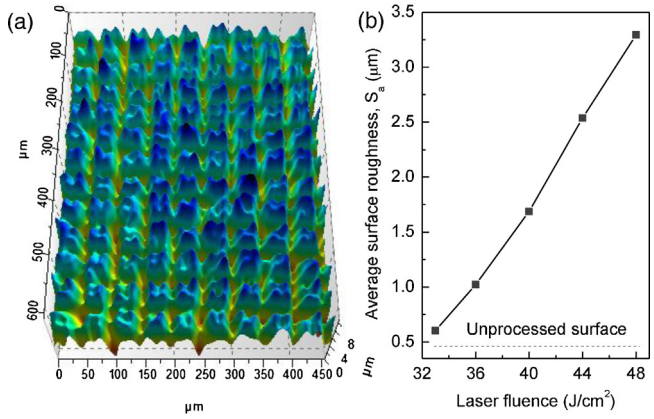

Fig. 3. Surface morphology of structured surfaces irradiated with same line separation of 50 μm and various powers. (a) 3D profile of a typical surface under 36 J/cm^2. (b) Average roughness of textured surfaces as function of laser fluence.

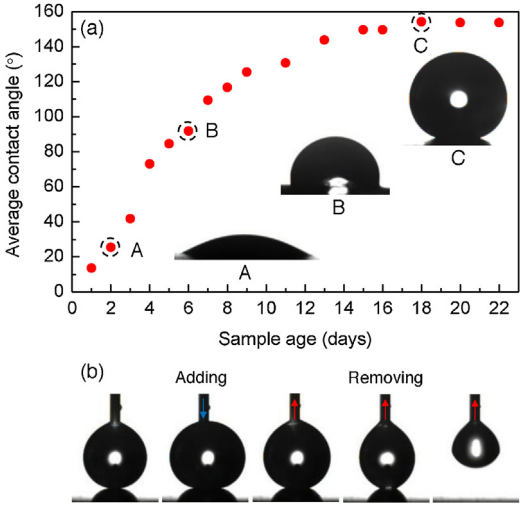

Fig. 4. Surface wettability evolution and contact angle hysteresis (CAH) measurement. (a) The contact angle of a droplet on a laser structured surface (a = 50 μm, fluence of 36 J/cm^2) develops with time. The inset shows droplet images measured after exposure to air for 2, 6 and 18 days. (b) The sequence of images indicates a growing/shrinking droplet. The sample was exposed to the air for 19 days.

For practical applications such as self-cleaning materials, a surface needs to have a small CAH, typically smaller than 10° [25]. The CAH can be measured by comparing the advancing and receding contact angles [11]. Fig. 4b demonstrates a sequence of droplet images (the completed process is presented in supporting video 1) where these two angles are determined. Firstly, a droplet was placed on the surface and then further filled with water. The droplet became bigger and the contact area notably increased (second image). This presents the growing or advancing contact angle and was found to be ~156°. Secondly, water was continuously removed which decreases the droplet size and the contact area. Finally, the droplet departed from the surface (final image). The receding contact angle was obtained just before the contact was broken (fourth image) and determined to be ~152°. As a result, the CAH was ~4°. It is noted that the droplet did not wet the surface during the measurement. Due to the large contact angle (~154°) and small CAH (~4°), the laser textured surfaces (after exposure to the air for 18 days or longer) are superhydrophobic [25], which make them attractive for a number of applications [26].

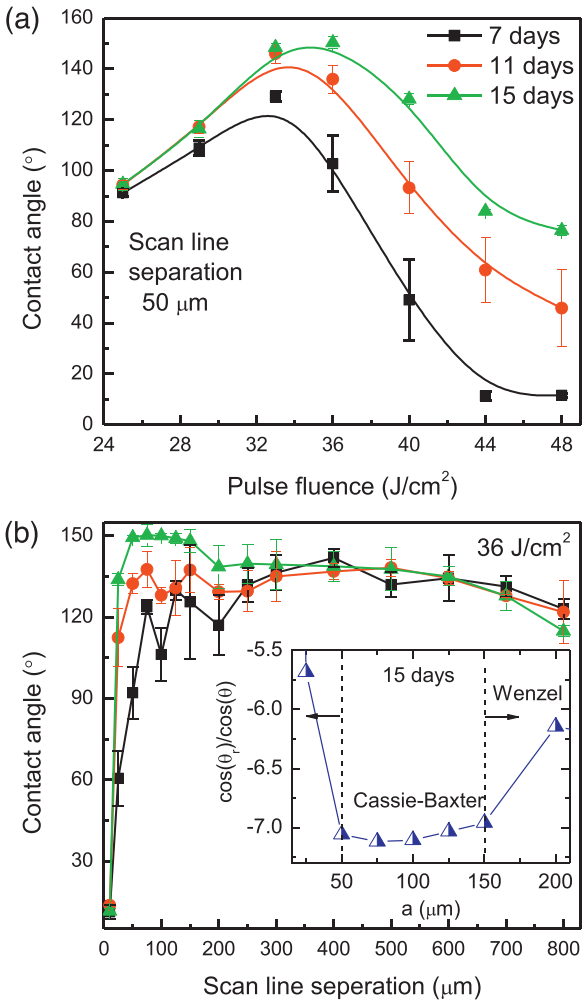

Fig. 5. Effect of laser fluence and line separation on wettability of laser structured surfaces. All examples were studied after exposure to the air for 7, 11, and 15 days. (a) The contact angle of surfaces with a 50 μm line separation and irradiated with various fluences. (b) The contact angle of surfaces irradiated with a fixed fluence of 36 J/cm^2 versus line separation. The error bars are the standard deviation of the average of three individual measurements per point. The inset presents the ratio between the cosine of contact angle (θ_r) of the laser textured surface (exposed to the air for 15 days) and the cosine of the contact angle ($\theta \sim 83^\circ$) of the as-received substrate as a function of line separation.

3.3. *Effect of laser power and scan line separation on surface wettability*

Laser power and structure have direct impacts on the wettability of textured surfaces. Below, these two factors are investigated separately, from which optimized fabrication parameters are given.

The laser power strongly affects surface morphology of the textured surface so it should influence the surface wettability. To study this effect, the samples were processed with the same line separation of 50 μm. Fig. 5a shows the contact angle of the processed surfaces as a function of fluence, expressing a similar curve when measured at different times after processing. As the laser power increases, the contact angle grows up to a maximum value and then gradually decreases. The optimized fluences for the given ~5 μL volume droplets, in order to achieve non-wettability in the shortest time after fabrication were 33 and 36 J/cm^2.

As can be seen in Fig. 3b, the surface roughness created was low for the fluence of 25 and 29 J/cm^2 hence the evolution of contact angle on the processed surfaces was not as pronounced compared with as-received surfaces. In contrast, for the high fluences (44 and 48 J/cm^2), the increased roughness enhanced the wettability. Also, as the amount of activated sites increases on the surface, it requires more time for the relevant reactions with air to render the high contact angle. For the fluences (33 and 36 J/cm^2), the roughness value was in between the two above cases, which allows for the development of superhydrophobicity in a reasonable time.

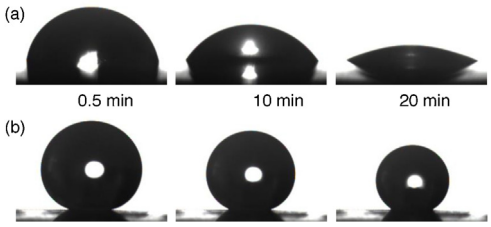

Fig. 6. Profile of a ~5 μL droplet on solid substrates over time. (a) The hydrophilic surface, the stainless steel sheet as supplied. (b) The superhydrophobic surface, a = 50 μm, was irradiated with 36 J/cm^2 and exposed to the air for 20 days.

To study the effect of scan line separation on the surface wettability, the laser fluence of 36 J/cm^2 was used for all samples. Fig. 5b plots the development of the contact angle versus the line spacing where the relationship can be divided into three main parts. The contact angle was very low, ~10°, for the smallest spacing of 10 μm and was moderate, ~130°, for the large spacing (a > 200 μm). In addition, for both cases, the contact angle did not show a significant change over 15 days. The most interesting event was observed for the medium separation of 25–200 μm where the evolution of contact angle with time was obvious. The contact angle at day 15 was generally higher than 130°, and especially, reached ~150° for a = 50–150 μm. SEM images of these surfaces with scan line separations from 75 to 150 μm are shown in Fig. S2. Furthermore, surfaces with a = 50–150 μm and after exposure to the air for 15 days or longer, exhibit incomplete wetting. The droplet did not wet these surfaces so the contact angle is described by Cassie-Baxter [5] rather than Wenzel's model [4]. The inset of Fig. 5b shows that at day 15, surface wettability of textured surfaces is at Wenzel's regime for a < 50 μm, changes to Cassie-Baxter for a = 50 μm and stays at this regime until a = 150 μm, and finally back to Wenzel's regime for a > 150 μm. As a result, the most suitable spacing for achieving incomplete wetting surfaces in the shortest exposure time is 50–150 μm.

It is noted that for a = 200 μm or larger, the increase of the scanning line distance results in surfaces with a significant portion untreated which has a negative effect on the contact angle and CAH. These surfaces did not become superhydrophobic even after being left under ambient air for several months. In contrast, laser processed surfaces with a = 10 and 25 μm became superhydrophobic after exposure to air for ~1 month.

3.4. *Evaporation of droplets*

It is well-known that evaporation flux strongly influences the development of the coffee-stain effect [24]. Fig. 6 compares the droplet profile for an initially ~2.2 mm diameter droplet on a superhydrophobic and the as-received surface over 20 min. The contact line of the droplet on the hydrophilic substrate is about three times larger in diameter than that of the droplet on non-wetting surface. The contact angle of the droplet on the hydrophilic surface decreased sharply 71%, from ~77° to 22°, which is nearly five times higher than the change of 15% (from ~154° to 130°) for the non-wetting surface.

Following the above observation, Fig. 7a and b depict the evaporation and shrinking of droplets when drying on non-wetting and wetting surfaces. For the hydrophilic surface, the evaporation flux is higher at the edge than at the droplet centre. As a result, the

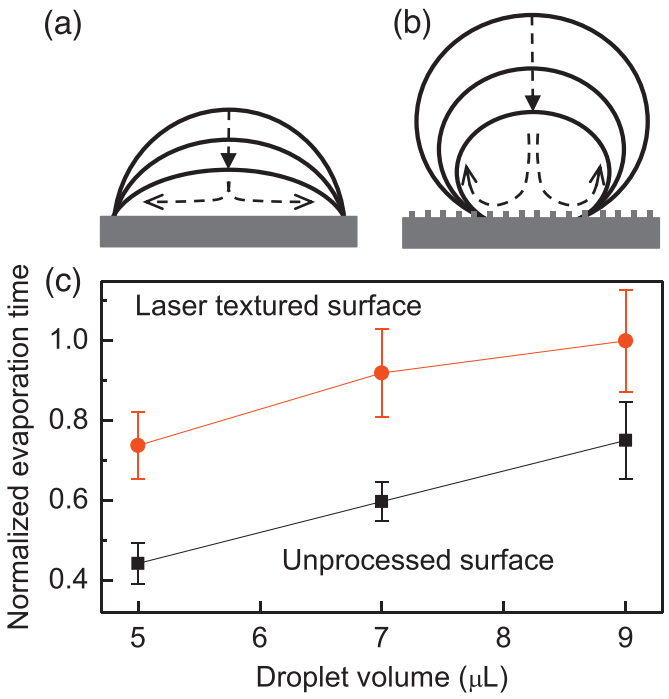

Fig. 7. Comparison of profile, evaporation flux, and evaporation time between droplets. Deposited on (a) the as-received and (b) superhydrophobic surfaces. The dashed-arrows represent capillary flows inside droplet. (c) Normalized evaporation time as a function of droplet volume.

fluid flows from the droplet centre to the contact line, resulting in the coffee-stain effect [27]. In contrast, as the droplet has a near spherical shape on the hydrophobic surface, the evaporation flux is expected to be highly uniform across the droplet surface. Furthermore, due to the small CAH (~4°) the contact line appears to be relatively free moving. As a result, fluid flows towards and then away from the edge so the coffee-stain effect is unlikely to be observed [28].

Average evaporation flux of the droplet on the hydrophilic substrate should be higher compared with that on the incomplete wetting surface. The total evaporation time (t_f) (measured from the time when a droplet is deposited on a surface until the evaporation is complete) of droplets with various volumes was investigated and is shown in Fig. 7c. Indeed, compared to the as-received surface, droplets on the non-wetting surfaces need about 1.5 times longer to completely evaporate.

3.5. Formation and prevention of the coffee-stain effect

Fig. 8a shows a sequence water droplet carrying PS particles that dries on the as-received substrates over time (the complete process is shown in the video 2). The transformation of the particles from droplet center to the rim can be seen clearly from the time when $t/t_f = 0.9$. Finally, when the evaporation is complete ($t/t_f = 1$), it leaves the ring-like stain with a diameter of around 3.2 mm. This so-called coffee-stain effect has been well-studied [24,29]. In some instances, this phenomenon is useful such as for fabrication of conducting lines [30] and particle separation [31].

However, the coffee-stain effect is undesirable in many applications including ink-jet printing [32,33] and biotechnology [34,35] as it causes non-uniform deposition. A number of techniques have been proposed in order to improve spot homogeneity, which can be classified into two groups. The first approach is using external factors such as temperature [32], electrowetting [36] and alternating current signal [37]. The second method is based on modification of the liquid [27,33], its suspended particles [38] and the substrate (hydrophilic or hydrophobic) used [39,40]. This work demonstrates that there is no coffee-stain effect on a superhydrophobic surface.

Fig. 8b shows a droplet (volume ~5 μL) drying on a superhydrophobic surface with time (more information is given in the video 3). After the evaporation is complete, uniform PS deposition with a near circular shape was obtained. The film diameter was ~1 mm, which is more than 3 times smaller than the size of the ring on the wetting surface. Fig. 8c and d compare surface morphology of the ring and the spot film. It is clear that most PS particles were deposited in the contact line on the hydrophilic surface but were uniformly distributed on the non-wetting surface. The result demonstrates that surfaces exhibiting hydrophobicity can provide a solution for achieving uniform coatings deposit from suspensions and can improve ink-jet printing resolution [32]. The formation of

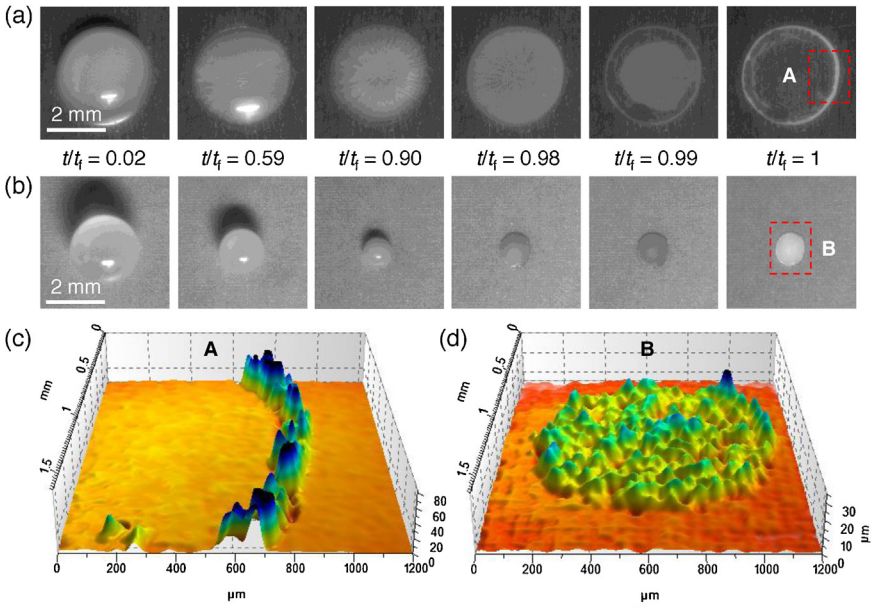

Fig. 8. Formation of the coffee-stain and uniform deposition. Transportation of particles in ~5 μL droplet on (a) as-received surfaces and (b) superhydrophobic ($a = 50$ μm, 36 J/cm^2 and exposed to the air for 15 days) over time. (c, d) 3D profile of the deposited material after droplet evaporation shown in (a, b), respectively.

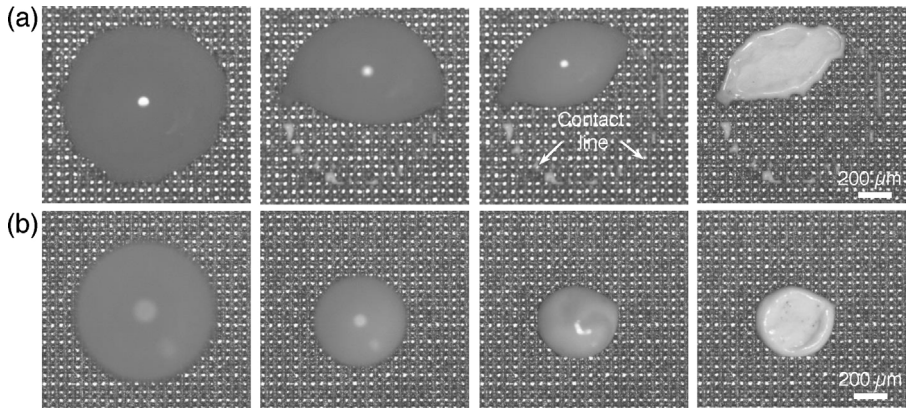

Fig. 9. Transportation of particles carried in a 5 μL droplet on superhydrophobic surfaces during evaporation. The contact line between the droplet and solid surface was moved to minimize the particle deposition. The two samples have $a = 50$ μm, irradiated with 36 J/cm^2 and were exposed to the air for (a) 22 and (b) 34 days. Images were captured using the Leica microscope.

uniform spots with a high density of nanoparticles also has potential for photonic device fabrication such as novel laser sources [41].

The area over which material is deposited on the superhydrophobic surface can be further reduced when the droplet contact line moves toward droplet centre. This effect is possible because of the creation of saturated vapor near the contact line during the drying process [42]. In our work, contact line movement was observed by increasing the evaporation flux (achieved by increasing the temperature of the surrounding air by ~4 °C). Fig. 9a clearly shows the movement of the initial contact line of a droplet on a 22-day old sample during the drying process. It is noticeable because a few PS particles were pinned on the contact line, forming a ring-like structure with diameter of 1 mm (similar to the observation in Fig. 8b). Most of PS particles were concentrated in an ellipse-like film (0.5 mm by 0.7 mm) located inside and at the top-left of the ring. Fig. 9b indicates that droplets on the 34-day old surface did not exhibit initial partial contact line pinning as after evaporation is complete there is no evidence of PS particles outside the central region. This is because the contact line was free moving so there were no PS particles pinned. All PS particles were concentrated in a spot with a diameter of about 0.5 mm, which is 2 times smaller compared with that (1 mm) observed in Fig. 8b. Compared with the original ring-like stain (shown in Fig. 8a), the area over which material has been deposited has been reduced by about 40 times. These finding should be very useful for controlling evaporative droplets carrying biological molecules or analyzers such as DNA, proteins and cells in which minimizing the patterned area is strongly desired [1]. It is noted that the PS particles are well adhered to the surface after the evaporation is complete.

4. Conclusions

It has been demonstrated that superhydrophobic surfaces on a common stainless steel can be fabricated by using a cost-effective and compact nanosecond laser system. Despite the processed surfaces exhibiting hydrophilic properties directly after fabrication, their wettability changes over time under ambient conditions and becomes non-wetting after 13 days. Optimized fabrication parameters are studied by investigation of the effect of laser power and scan line separation on surface wettability of textured surfaces. Interestingly, the syperhydrophobic surfaces can be employed for achieving spot homogeneity. Droplets with PS suspended particles on the as-received surface form clear, non-uniform ring-like structures after evaporation is complete. Conversely, on the incomplete wetting surfaces uniform deposition of the PS is observed. For the same droplet volume, the deposited area of the PS particles on the laser textured surfaces is one order of magnitude smaller compared with that on the unprocessed surface. This finding is useful for biological applications, in which minimizing the deposition of DNA, proteins and cell suspensions is highly important, as well as advanced fabrication techniques for uniform coatings and high resolution ink-jet prints.

Data availability All relevant data present in this publication can be accessedat http://dx.doi.org/10.17861/a24ec3ae-acbe-4c23-9793-fa24648a6ce6

Acknowledgements

We thank Dr. Jim Buckman for helping with SEM and EDX measurements. This work is funded by the UK Engineering and Physical Sciences Research Council under grants EP/L017431/1, EP/L017350/1, EP/L016907/1 and EP/L017415/1.

Appendix A. Supplementary data

Supplementary material related to this article can be found, in the online version, at http://dx.doi.org/10.1016/j.apsusc.2016.01.019.

References

[1] R. Blossey, Self-cleaning surfaces-virtual realities, Nat. Mater. 2 (2003) 301–306.
[2] N.J. Shirtcliffe, G. McHale, S. Atherton, M.I. Newton, An introduction to superhydrophobicity, Adv. Colloid Interface Sci. 161 (2010) 124–138.
[3] B. Bhushan, Y.C. Jung, Natural and biomimetic artificial surfaces for superhydrophobicity, self-cleaning, low adhesion, and drag reduction, Prog. Mater. Sci. 56 (2011) 1–108.
[4] R.N. Wenzel, Resistance of solid surfaces to wetting by water, Ind. Eng. Chem. 28 (1936) 988–994.
[5] A.B.D. Cassie, S. Baxter, Wettability of porous surfaces, Trans. Faraday Soc. 40 (1944) 0546–0550.
[6] Y.Y. Yan, N. Gao, W. Barthlott, Mimicking natural superhydrophobic surfaces and grasping the wetting process: a review on recent progress in preparing superhydrophobic surfaces, Adv. Colloid Interface Sci. 169 (2011) 80–105.
[7] F. Chen, D. Zhang, Q. Yang, J. Yong, G. Du, J. Si, F. Yun, X. Hou, Bioinspired wetting surface via laser microfabrication, ACS Appl. Mater. Interfaces 5 (2013) 6777–6792.
[8] A.Y. Vorobyev, C.L. Guo, Direct femtosecond laser surface nano/microstructuring and its applications, Laser Photon. Rev. 7 (2013) 385–407.
[9] M. Jin, X. Feng, J. Xi, J. Zhai, K. Cho, L. Feng, L. Jiang, Super-hydrophobic PDMS surface with ultra-low adhesive force, Macromol. Rapid Commun. 26 (2005) 1805–1809.
[10] A. Dunn, J.V. Carstensen, K.L. Wlodarczyk, E.B. Hansen, J. Gabzdyl, P.M. Harrison, J.D. Shephard, D.P. Hand, Nanosecond laser texturing for high friction applications, Opt. Lasers Eng. 62 (2014) 9–16.
[11] M. Groenendijk, Fabrication of super hydrophobic surfaces by fs laser pulses, Laser Technol. 5 (2008) 44–47.

[12] A.-M. Kietzig, S.G. Hatzikiriakos, P. Englezos, Patterned superhydrophobic metallic surfaces, Langmuir 25 (2009) 4821–4827.
[13] D.L. Tian, Y.L. Song, L. Jiang, Patterning of controllable surface wettability for printing techniques, Chem. Soc. Rev. 42 (2013) 5184–5209.
[14] J.D.J.S. Samuel, P. Ruther, H.P. Frerichs, M. Lehmann, O. Paul, J. Rühe, A simple route towards the reduction of surface conductivity in gas sensor devices, Sens. Actuator B-Chem. 110 (2005) 218–224.
[15] B. Wu, M. Zhou, J. Li, X. Ye, G. Li, L. Cai, Superhydrophobic surfaces fabricated by microstructuring of stainless steel using a femtosecond laser, Appl. Surf. Sci. 256 (2009) 61–66.
[16] P. Bizi-Bandoki, S. Benayoun, S. Valette, B. Beaugiraud, E. Audouard, Modifications of roughness and wettability properties of metals induced by femtosecond laser treatment, Appl. Surf. Sci. 257 (2011) 5213–5218.
[17] R. Jagdheesh, B. Pathiraj, E. Karatay, G. Romer, A.J.H. in't Veldt, Laser-induced nanoscale superhydrophobic structures on metal surfaces, Langmuir 27 (2011) 8464–8469.
[18] P. Bizi-bandoki, S. Valette, E. Audouard, S. Benayoun, Time dependency of the hydrophilicity and hydrophobicity of metallic alloys subjected to femtosecond laser irradiations, Appl. Surf. Sci. 273 (2013) 399–407.
[19] A. Cunha, A.P. Serro, V. Oliveira, A. Almeida, R. Vilar, M.-C. Durrieu, Wetting behaviour of femtosecond laser textured Ti–6Al–4V surfaces, Appl. Surf. Sci. 265 (2013) 688–696.
[20] S. Moradi, S. Kamal, P. Englezos, S.G. Hatzikiriakos, Femtosecond laser irradiation of metallic surfaces: effects of laser parameters on superhydrophobicity, Nanotechnology 24 (2013) 415302.
[21] M.V. Rukosuyev, J. Lee, S.J. Cho, G. Lim, M.B.G. Jun, One-step fabrication of superhydrophobic hierarchical structures by femtosecond laser ablation, Appl. Surf. Sci. 313 (2014) 411–417.
[22] A.Y. Vorobyev, C. Guo, Multifunctional surfaces produced by femtosecond laser pulses, J. Appl. Phys. 117 (2015) 033103.
[23] D.V. Ta, A. Dunn, T.J. Wasley, R.W. Kay, J. Stringer, P.J. Smith, C. Connaughton, J.D. Shephard, Nanosecond laser textured superhydrophobic metallic surfaces and their chemical sensing applications, Appl. Surf. Sci. 357 (2015) 248–254.
[24] R.D. Deegan, O. Bakajin, T.F. Dupont, G. Huber, S.R. Nagel, T.A. Witten, Capillary flow as the cause of ring stains from dried liquid drops, Nature 389 (1997) 827–829.
[25] J. Drelich, E. Chibowski, D.D. Meng, K. Terpilowski, Hydrophilic and superhydrophilic surfaces and materials, Soft Matter 7 (2011) 9804–9828.
[26] L. Feng, S. Li, Y. Li, H. Li, L. Zhang, J. Zhai, Y. Song, B. Liu, L. Jiang, D. Zhu, Super-hydrophobic surfaces: from natural to artificial, Adv. Mater 14 (2002) 1857–1860.
[27] M. Majumder, C.S. Rendall, J.A. Eukel, J.Y.L. Wang, N. Behabtu, C.L. Pint, T.-Y. Liu, A.W. Orbaek, F. Mirri, J. Nam, A.R. Barron, R.H. Hauge, H.K. Schmidt, M. Pasquali, Overcoming the "Coffee-Stain" effect by compositional marangoni-flow-assisted drop-drying, J. Phys. Chem. B 116 (2012) 6536–6542.
[28] H. Masoud, J.D. Felske, Analytical solution for Stokes flow inside an evaporating sessile drop: spherical and cylindrical cap shapes, Phys. Fluids 21 (2009) 042102.
[29] H. Hu, R.G. Larson, Marangoni effect reverses coffee-ring depositions, J. Phys. Chem. B 110 (2006) 7090–7094.
[30] S. Magdassi, M. Grouchko, D. Toker, A. Kamyshny, I. Balberg, O. Millo, Ring stain effect at room temperature in silver nanoparticles yields high electrical conductivity, Langmuir 21 (2005) 10264–10267.
[31] T.-S. Wong, T.-H. Chen, X. Shen, C.-M. Ho, Nanochromatography driven by the coffee ring effect, Anal. Chem. 83 (2011) 1871–1873.
[32] D. Soltman, V. Subramanian, Inkjet-printed line morphologies and temperature control of the coffee ring effect, Langmuir 24 (2008) 2224–2231.
[33] J. Park, J. Moon, Control of colloidal particle deposit patterns within picoliter droplets ejected by ink-jet printing, Langmuir 22 (2006) 3506–3513.
[34] R. Blossey, A. Bosio, Contact line deposits on cDNA microarrays: a "twin-spot effect", Langmuir 18 (2002) 2952–2954.
[35] V. Dugas, J. Broutin, E. Souteyrand, Droplet evaporation study applied to DNA chip manufacturing, Langmuir 21 (2005) 9130–9136.
[36] H.B. Eral, D.M. Augustine, M.H.G. Duits, F. Mugele, Suppressing the coffee stain effect: how to control colloidal self-assembly in evaporating drops using electrowetting, Soft Matter 7 (2011) 4954–4958.
[37] J. Mu, P. Lin, Q. Xia, Concentric rings of polystyrene and titanium dioxide nanoparticles patterned by alternating current signal guided coffee ring effect, Appl. Phys. Lett. 104 (2014) 261601.
[38] P.J. Yunker, T. Still, M.A. Lohr, A.G. Yodh, Suppression of the coffee-ring effect by shape-dependent capillary interactions, Nature 476 (2011) 308–311.
[39] Y. Kim, G.B. Hurst, M.J. Doktycz, M.V. Buchanan, Improving spot homogeneity by using polymer substrates in matrix-assisted laser desorption/ionization mass spectrometry of oligonucleotides, Anal. Chem. 73 (2001) 2617–2624.
[40] Y.-F. Li, Y.-J. Sheng, H.-K. Tsao, Evaporation stains: suppressing the coffee-ring effect by contact angle hysteresis, Langmuir 29 (2013) 7802–7811.
[41] Y. Wang, K.E. Fong, S. Yang, Van D. Ta, Y. Gao, Z. Wang, V. Nalla, H.V. Demir, H. Sun, Unraveling the ultralow threshold stimulated emission from CdZnS/ZnS quantum dot and enabling high-Q microlasers, Laser Photon. Rev. 9 (2015) 507–516.
[42] G. McHale, S.M. Rowan, M.I. Newton, M.K. Banerjee, Evaporation and the wetting of a low-energy solid surface, J. Phys. Chem. B 102 (1998) 1964–1967.